Am J Physiol Cell Physiol 299: C977–C987, 2010.
First published August 4, 2010; doi:10.1152/ajpcell.00377.2009.

Microfibrils and fibrillin-1 induce integrin-mediated signaling, proliferation and migration in human endothelial cells

Boubacar Mariko,[1] Zeinab Ghandour,[1] Stéphanie Raveaud,[1] Mickaël Quentin,[1] Yves Usson,[2] Jean Verdetti,[1] Philippe Huber,[1] Cay Kielty,[3,4] and Gilles Faury[1]

[1]*Laboratoire "Physiopathologies Vasculaires: Interactions Cellulaires, Signalisation et Vieillissement," Université Joseph Fourier, CEA; Institut National de la Santé et de la Recherche Médicale, U882, Grenoble;* [2]*Laboratory TIMC, Team "Reconnaissance des Formes et Microscopie Quantitative," Institut d'Ingéniérie et de l'Information de Santé, Centre National de la Recherche Scientifique, UMR5525, Grenoble; Université Joseph Fourier, La Tronche, France;* [3]*Wellcome Trust Centre for Cell-Matrix Research, and* [4]*Centre for Tissue Regeneration, University of Manchester, Manchester, United Kingdom*

Submitted 20 August 2009; accepted in final form 27 July 2010

Mariko B, Ghandour Z, Raveaud S, Quentin M, Usson Y, Verdetti J, Huber P, Kielty C, Faury G. Microfibrils and fibrillin-1 induce integrin-mediated signaling, proliferation and migration in human endothelial cells. *Am J Physiol Cell Physiol* 299: C977–C987, 2010. First published August 4, 2010; doi:10.1152/ajpcell.00377.2009.—Microfibrils are macromolecular complexes associated with elastin to form elastic fibers that endow extensible tissues, such as arteries, lungs, and skin, with elasticity property. Fibrillin-1, the main component of microfibrils, is a 350-kDa glycoprotein for which genetic haploinsufficiency in humans can lead to Marfan syndrome, a severe polyfeatured pathology including aortic aneurysms and dissections. Microfibrils and fibrillin-1 fragments mediate adhesion of several cell types, including endothelial cells, while fibrillin-1 additionally triggers lung and mesangial cell migration. However, fibrillin-1-induced intracellular signaling is unknown. We have studied the signaling events induced in human umbilical venous endothelial cells (HUVECs) by aortic microfibrils as well as recombinant fibrillin-1 Arg-Gly-Asp (RGD)-containing fragments PF9 and PF14. Aortic microfibrils and PF14, not PF9, substantially and dose dependently increased HUVEC cytoplasmic and nuclear calcium levels measured using the fluorescent dye Fluo-3. This effect of PF14 was confirmed in bovine aortic endothelial cells. PF14 action in HUVECs was mediated by $\alpha v\beta 3$ and $\alpha 5\beta 1$ integrins, phospholipase-C, inositol 1,4,5-trisphosphate, and mobilization of intracellular calcium stores, whereas membrane calcium channels were not or only slightly implicated, as shown in patch-clamp experiments. Finally, PF14 enhanced endothelial cell proliferation and migration. Hence, fibrillin-1 sequences may physiologically activate endothelial cells. Genetic fibrillin-1 deficiency could alter normal endothelial signaling and, since endothelium dysfunction is an important contributor to Marfan syndrome, participate in the arterial anomalies associated with this developmental disease.

adhesion; calcium signaling; Marfan syndrome

LARGE ARTERIES have an essential mechanical role in the smoothing of the pulsatile blood flow and pressure during the cardiac cycle. This function is made possible by extracellular elastic components of the arterial wall. In many invertebrates, with an open and low pressure circulatory system, arterial elasticity is mainly provided by microfibrils, a supramolecular assembly of more than 17 proteins, including fibulins, emilins, latent transforming growth factor-β (TGF-β) binding proteins (LTBPs), and fibrillins (16, 26, 34). Microfibrils and fibrillins were rather conserved during evolution and present clear similarities between invertebrate and vertebrates (9, 55, 65). In vertebrates, arterial elasticity, more adapted to the close and high-pressure circulatory system, is provided by elastic fibers made of elastin (90%, only present in vertebrates) and microfibrils (10%) (58). Elastin is the main contributor to the elastic properties of these fibers, although microfibrils moderately participate in the elastic fiber mechanics (43). As a consequence, elastin or fibrillin-1 haploinsufficiency induces arterial mechanics alteration and remodelling (18, 42, 45, 52). During development of elastic tissues, microfibrils are the first elastic fiber structure that is formed. Tropoelastin, the precursor of elastin, is then deposited on the microfibril scaffold before molecular rearrangement, which leads to the mature/functional elastic fiber (34, 75).

Besides their mechanical role, microfibrils and microfibrillar components can also be involved in cell adhesion. In the developing aorta, microfibrils/fibrillin come in direct contact with endothelial cells (by passing through the basement membrane) and smooth muscle cells and mediate the anchoring of these cells to the internal elastic lamina (13, 14). The anchoring activity of microfibrils seems to be mediated at least in part by their main component fibrillin-1, since *1*) fibrillin-1 domains extend out of microfibrils (38) and *2*) besides modulating extracellular matrix synthesis and deposition, fibrillin-1 fragments mediate adhesion and spreading of several cell types in vitro, including fibroblasts, smooth muscle cells, and endothelial cells (5, 53, 61, 70).

Fibrillin-1 is a 350-kDa cystein-rich glycoprotein that has first been characterized in humans, mice, and chickens (60, 75). Autosomal dominant mutations in the fibrillin-1 gene can be responsible for the human genetic disorder Marfan Syndrome (MFS), which features, at the vascular level, aneurysms and aortic disruptions (32, 46). One of the pleiotropic causes of MFS seems to be endothelial dysfunction, since it has been observed in these patients: *1*) reduced flow-mediated vasodilation, suggesting an altered endothelial cell signaling, and *2*) elevated plasma levels of homocysteine, which attenuate endothelial function and limits nitric oxide (NO) bioavailability (22, 30, 71). The participation of fibrillin-1 in endothelial cell anchoring together with the observation of an endothelial detachment in fibrillin-1 null mice ($Fbn1^{-/-}$), a mouse model for MFS (11), suggests that binding of fibrillin-1 to the endothelial cell is important in arterial morphogenesis and physiology. Alteration of this interaction may be one of the causes of

Address for reprint requests and other correspondence: G. Faury, LAPV/INSERM U882, iRTSV, CEA-Grenoble, 17 rue des Martyrs, 38054 Grenoble cedex 9, France (e-mail: Gilles.Faury@ujf-grenoble.fr).

the vascular dysfunctions and remodelling observed in MFS. To support these hypotheses, it has been found that the Arg-Gly-Asp (RGD) motif in the fourth TGFβ-binding protein-like domain of human fibrillin-1 is flexible and accessible and regulates cell adhesion and spreading through binding to integrins (40). The integrins involved are, in particular, $\alpha_v\beta_3$ or $\alpha_5\beta_1$ in fibroblasts and β_1-subunit in smooth muscle cells (5, 53, 61) and the subunits α_v, α_5, and β_1 in endothelial cells (70). However, the signaling mechanisms directly induced by fibrillin-1 in endothelial cells are unknown. Since endothelial integrins and intracellular calcium level play an important role during embryonic development and angiogenesis (50, 64), we have investigated here the potential integrin-mediated signaling events and functions triggered by microfibrils and fibrillin-1 fragments in human endothelial cells.

MATERIALS AND METHODS

A more detailed materials and methods is also provided as online supporting information.

Cell Culture

Human umbilical venous endothelial cells (HUVEC) were isolated using a technique adapted from Jaffe et al. (19, 29). Cells were harvested from the umbilical vein by a 10-min incubation at 37°C with collagenase 1A and cultured in 0.25 mg/ml human fibronectin-coated dishes in medium 199 containing 22% human serum, streptomycin (0.1 mg/ml), penicillin (100 UI/m), and L-glutamine (2 mmol/l). Umbilical cords were harvested after birth, with full informed consent of the mother, according to the French government order no. 2007-1220 from August 10, 2007. Each cell culture was prepared by pooling the endothelial cells from two to three umbilical cords. Bovine aortic endothelial cells (BAEC) were prepared by collagenase treatment of bovine aorta, as described previously (3).

Production of Aortic Microfibrils and Fibrillin-1 Fragments

Microfibrils were isolated from bovine aorta, in native and nondenaturing conditions, as previously described (4, 15, 38, 10, 44). A piece of the aorta from a newborn calf was incubated for 18 h at 4°C with 0.5 mg/ml purified bacterial collagenase 1A, in the presence of hyaluronidase (5 U/ml) and freshly prepared protease inhibitors. In both cases, segments of bovine aortas were collected at the slaughterhouse immediately after the animal's death. Microfibrils were collected after passage of the supernatant through a CL-2B sepharose column and purified by CsCl density gradient centrifugation. In our experiments, aortic microfibrils (average molecular mass ≈ 15,000 kDa) were used at 0.15 μg/ml ($\approx 10^{-11}$ mol/l), 0.5 μg/ml ($\approx 3.3 \times 10^{-11}$ mol/l), and 1.5 μg/ml ($\approx 10^{-10}$ mol/l).

The cloning, expression, and purification of RGD-containing recombinant human fibrillin-1 fragments PF9 (residues 1528–1807) and PF14 (residues 1362–1688), using the mammalian expression vector pCEP-pu/AC7 and 293-EBNA cells, has been described (5, 6). The domains of the fibrillin-1 fragments are presented in the online supporting information.

RGD-RGA PF14 mutant (PF14-RGA) was produced using a site-directed mutagenesis of aspartic acid 1541 to alanine, as described (6). Validation of the purity and folding of all the fragments used were performed, as described (6).

$[Ca^{2+}]_i$ in Adhering HUVEC

Measurements and analyses were performed either by confocal laser scanning microscopy (Zeiss LSM 410, Carl Zeiss, Iena, Germany) or by classical microscopy (CellR system, Olympus, Rungis, France) using the calcium-sensitive fluorescent dye Fluo-3/AM (excitation: 488 nm; emission: >510 nm, purchased from Sigma-Aldrich, St. Quentin-Fallavier, France), according to the previously described procedures (19). The cells were bathed in a physiological salt solution composed of (in mmol/l) 125 NaCl; 5.6 KCl, 2.4 $CaCl_2$, 1.2 $MgCl_2$, 11 D-glucose, and 10 HEPES; pH 7.4. In the figures, each tracing represents Fluo-3 fluorescence in one cell. Bradykinin, a reference agent elevating intracellular free calcium concentration ($[Ca^{2+}]_i$) in endothelial cells, was used to verify cell functionality. In some experiments, 10 μg/ml LM609 or JBS5 blocking antibodies (Chemicon Europe, Southampton, UK) to integrins $\alpha_v\beta_3$ or $\alpha_5\beta_1$, respectively, were applied to HUVECs 30 min before the addition of PF14 and during the experiment.

Other experiments were conducted using the calcium-sensitive dye Fura-2 (Sigma-Aldrich) in place of Fluo-3, to obtain actual intracellular calcium concentrations. The loading and analysis procedures were previously described (17).

Electrophysiological Recording

Calcium current recordings (imposed potential: +20 mV) were performed using the cell-attached patch-clamp technique (single channel) and materials previously described (19). Cells were immerged in a Tyrode solution containing (in mmol/l) 125 NaCl, 5.6 KCl, 2.4 $CaCl_2$, 1.2 $MgCl_2$, 10 HEPES, and 11 glucose, pH 7.4. The patch pipette was filled with a solution containing $Ba(CH3COO)_2$ (90 mmol/l) and HEPES (10 mmol/l), pH 7.4. Resting potential (V_m) equals -57 ± 4 mV ($n = 35$) for nondividing cells (19). The recorded transmembrane currents were integrated and analyzed using the software Biopatch (Biologic, Claix, France).

siRNA Knockdown of Integrin Subunits αv and α5

siRNA synthesis. Control and α5 integrin small interfering RNAs (siRNAs) were purchased as four oligonucleotide Smart Pools (Dharmacon, Lafayette, CO). siRNAs targeting αv integrin were designed using DSIR algorithm (67) and synthesized by Dharmacon.

siRNA transfection. Confluent HUVECs were cultured at 8×10^5 cells in 60-mm diameter dishes for 24 h. Cells were then trypsinized and transfected with siRNAs at 1 nM using AMAXA as previously described (63). The subsequent decrease in α5 expression was assessed by immunoblotting (−72%, see Fig. 5*A*). αv is a protein difficult to substantially knock down (23), and one transfection with αv siRNAs only produced a limited extinction (−25%). Therefore, cells were transfected a second time with αv siRNAs 48 h after the first transfection. This led to a more significant extinction of αv (approximately equal to −71%), which was assessed by flow cytometry (see Fig. 5, *C* and *D*) since, despite the use of several commercial antibodies, αv immunoblotting never produced clearly specific bands. Transfected cells were then cultured in 35-mm diameter, fibronectin-coated, glass-bottom dishes and used for calcium measurement experiments.

Antibodies. Polyclonal rabbit antibody to integrin α5 and mouse monoclonal antibody to integrin αv were from Santa Cruz Biotechnology (Heidelberg, Germany). Monoclonal mouse antibody to anti-β-tubulin was from Sigma-Aldrich.

Cell lysis and Western blotting. HUVEC monolayer extracts were electroporated and then centrifuged at 15,000 *g* for 5 min at 4°C. Protein concentration of the lysates was then determined with a Micro-BCA kit (Pierce, Rockford, IL). After polyacrylamide gel electrophoresis of the protein and electroblotting onto nitrocellulose, the blots were incubated overnight (4°C) with the primary antibodies, rabbit anti-integrin α5, or anti-tubulin in blocking buffer. The antigen was then detected using the ECL kit (Amersham Pharmacia Biotech-GE Healthcare, Saclay, France) with a peroxidase-labeled goat anti-rabbit antibody.

Flow cytometry. Aliquots of 10^6 cells were centrifuged and resuspended in 1% fetal calf serum containing PBS in the presence of anti-αv-primary antibody and, after washing was completed, the cells

were incubated for 30 min with the secondary antibody. Cells were then pelleted, resuspended in 0.5 ml phosphate-buffered saline containing 1% BSA, and analyzed on a fluorescence-activated cell sorter analyzer (Becton Dickinson, Franklin Lakes, NJ). A fluorescence threshold separating the αv-negative cells (M1) from αv-positive cells (M2) was set using autofluorescence of unlabeled/untransfected cells as negative control. In each experiment, the relative αv content in cell populations was estimated as the product of the percentage of αv-positive cells (M2, see Fig. 5*C*, table, column head: "% Gated") by the mean αv content per αv-positive cell. The mean αv content per αv-positive cell is assumed to be represented by the mean fluorescence level per cell (M2, Fig. 5*C*, table, column head: "Mean") from which the mean autofluorescence of unlabeled cells (measured at a value of 12.9) was deducted. The value obtained for control siRNA-transfected cells was considered as the reference, normalized to a value of 100.

HUVEC adhesion assay. 96-Well microplates were coated with different concentrations of human plasma fibronectin and fibrillin-1 recombinant fragments (PF14 and PF9) and kept at 4°C overnight. BSA (10 mg/ml) was used as negative control. After the unbound peptides were removed, the nonspecific binding was blocked by 10 mg/ml BSA for 2 h at room temperature. HUVEC were trypsinized and seeded at 3×10^4 cells/well in serum-free medium and incubated for 1 h, 30 min at 37°C, 5%CO_2. Nonadherent cells were removed and adherent cells were fixed with 10% glutaraldehyde in Percoll for 5 min. The wells were washed with phosphate-buffered saline and stained with crystal violet 0.1% (wt/vol) in water for 30 min. The cells were washed with water and lysed in 0.2% Triton X-100 in water for 2 h. The absorbance was measured at 460 nm with an ELISA plate reader.

HUVEC Proliferation

Two different methods used were the following.

Trypsinization/cell count method. HUVEC were trypsinized and resuspended in deprivated culture medium containing 5% human serum to limit spontaneous cell proliferation. Two hours after cell seeding, the dishes were incubated with 1 μg/ml (≈26 nmol/l) PF14 or PF9, or solvent of these fibrillin-1 fragments. After 48 h, cells were trypsinized and counted using a Kova cell count unit. Proliferation rate was (Cell $number_{48h}$ − Cell $number_{0h}$) × 100/Cell $number_{0h}$.

WST-1 colorimetric method. The measurement is based on the ability of mitochondrial dehydrogenases of viable cells to cleave tetrazolium salts (2). Two hours after cell plating, HUVECs were treated with PF14 (1 μg/ml; ≈26 nmol/l) or solvent alone for 48 h. Cell proliferation reagent 4-[3-[4-iodophenyl]-2–4(4-nitrophenyl)]-2H-5-tetrazolio-1,3-benzene disulfonate (WST-1, 10 μl/well) (Roche Diagnostics, Meylan, France) was added. Absorbance of the samples, proportional to the viable cell number, was then measured after 3 h at 450 nm using a microplate reader, and background absorbance was deducted. Proliferation rate was (Absorbance$_{48h}$ − Absorbance$_{0h}$) × 100/Absorbance$_{0h}$.

Cell Migration/Haptotaxis-Transwell Assay

Cell migration was assayed using a modified Boyden chamber as previously described (39). The lower side of the transwell inserts (3 μm pore; Falcon, Becton-Dickinson) was previously coated overnight with PF14 and PF9 fragments at 10 μg/ml.

Confluent monolayer of HUVEC was labeled in serum-free medium 199 with CellTracker CMRA Orange (10 μM) for 45 min at 37°C. Cells were rinsed and incubated in fresh medium for an additional 45 min at 37°C to allow leakage of unbound fluorophore.

Fluorophore-labeled HUVECs were trypsinized and suspended at the final concentration of 2×10^5 cells/ml in medium 199 containing 0.5% human serum. The cell suspension (100 μl) was added to the upper side of the transwell inserts. The inserts were placed in 24-well plates (Becton-Dickinson) containing 500 μl medium 199 with 0.5% human serum (control) and incubated at 37°C. The migration of cells through the optically opaque insert membrane to the lower chamber was measured by fluorescence measurement at 0 and 24 h. The fluorescence level difference between 0 and 24 h was representative of the number of migrated cells.

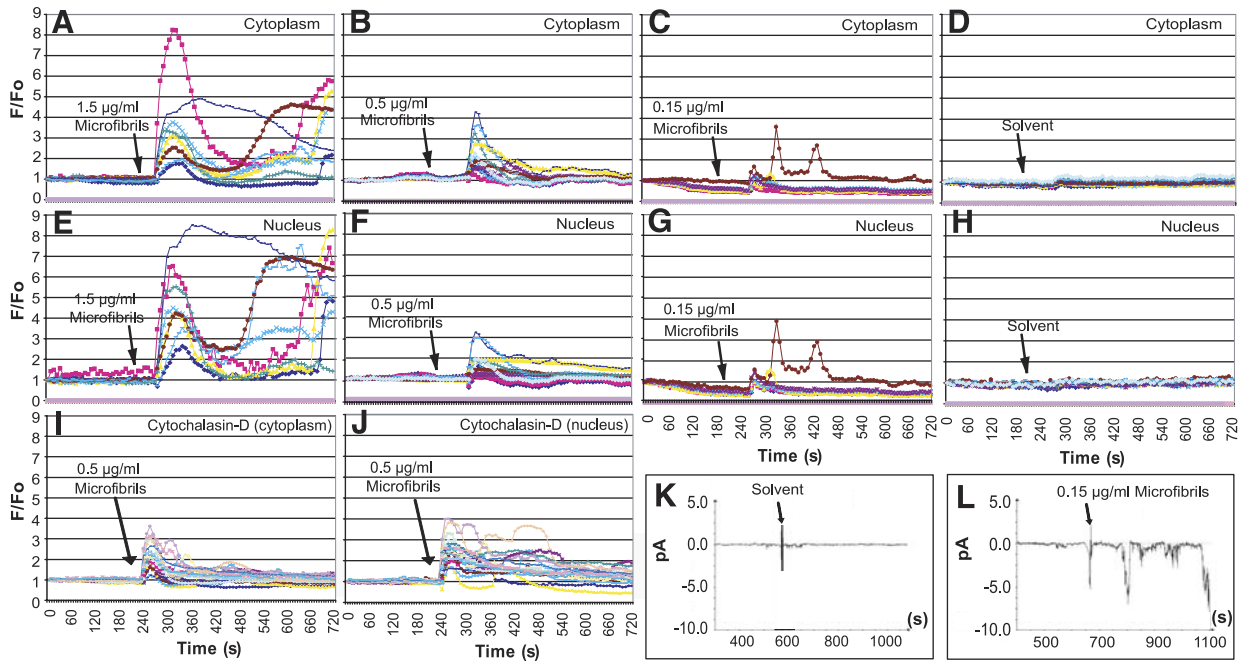

Fig. 1. Effect of aortic microfibrils on human umbilical venous endothelial cells (HUVEC) nuclear and cytoplasmic [Ca^{2+}]. *A–H*: dose effect of microfibrils. n = 27–30 cells (control: n = 56). *I*, *J*: effect of microfibrils (0.5 μg/ml) after 45 min incubation with cytochalasin-D (1 μmol/l) (n = 28 cells). *K*, *L*: microfibril-induced activation of membrane calcium channels recorded in patch-clamp experiments. All experiments were at least triplicated. Representative experiments are presented.

HUVEC Wound Healing Assay

This in vitro assay aims at evaluating the cellular proliferation and migration capabilities when some cells are destroyed in a confluent monolayer, leading to replacement of the missing cells. Wounds were produced in vitro by scratching the cell layer using a pipette tip, and wound closure was monitored over time as previously described (1). HUVECs were grown in human plasma fibronectin-coated plates until confluence in complete culture medium and then incubated in deprived culture medium (5% human serum instead of 22%) overnight. Cell cultures were imaged at 0 and 8 h after being wounded and after the addition of solvent, PF9, and PF14 (1 μg/ml). Wound areas were measured from the images using Image J software (NIH). Wound closure rate is (Wound $area_{0h}$ − Wound $area_{8h}$) × 100/Wound $area_{0h}$.

Data Analysis

When applicable, groups were compared by using one- or two-way ANOVAs followed by Fisher's Least Significant Difference test for paired comparisons, and presented values were means ± SE. $P \leq 0.05$ was considered as statistically significant.

RESULTS

Action of Microfibrils on $[Ca^{2+}]_i$

Addition of aortic microfibrils produced substantial, dose-dependent and transient elevations of Fluo-3 fluorescence in HUVEC cytoplasm and nucleus, indicative of free calcium level increases. The $[Ca^{2+}]$ elevations, present in most cells, were in the ranges of 1.3- to 8-fold at 1.5 μg/ml, 1.1- to 4-fold at 0.5 μg/ml, and 1- to 3-fold at 0.15 μg/ml microfibrils (Fig. 1, *A–H*). Regarding the cytoplasmic calcium rise, the effects of 1.5 μg/ml (peak mean value = 3.5 ± 0.3-fold) and 0.5 μg/ml microfibrils (peak mean value = 2.1 ± 0.1-fold) were significantly higher than those produced by 0.15 μg/ml microfibrils (peak mean value = 1.3 ± 0.1-fold) or the solvent alone (mean value = 1.1 ± 0.0-fold) (two-way ANOVA, $P \leq 0.05$). No significant difference could be detected between the effects of 0.15 μg/ml microfibrils and solvent. Regarding the nuclear calcium rise, the effects of 1.5 μg/ml, 0.5 and 0.15 μg/ml microfibrils (peak mean values = 4.9 ± 0.4, 2.1 ± 0.1, and 1.8 ± 0.2-fold, respectively) were significantly greater than those produced by the solvent alone (mean value = 1.2 ± 0.0-fold) (two-way ANOVA, $P \leq 0.05$).

Since microfibrils interact with integrins (5, 35), which are membrane receptors linked to actin microfilaments, we investigated the possibility of an actin-mediated transduction of the microfibrillar signal. After treatment of HUVEC with the actin-depolymerizer cytochalasin-D, the cells classically changed their morphology to a more spread phenotype. When 0.5 μg/ml microfibrils (an intermediate concentration high enough to trigger substantial raises in $[Ca^{2+}]_i$ and low enough to avoid a potential plateau effect of the high doses) was applied, cytochalasin-D-treated HUVEC had a response to similar to that of untreated cells; i.e., a 1.5- to 4-fold increase in both nuclear and cytoplasmic fluorescence. This indicated that actin microfilaments did not mediate the microfibril-induced $[Ca^{2+}]_i$ signaling in HUVECs (Fig. 1, *B*, *F*, *I*, and *J*).

The possibility of an involvement of Ca^{2+} channels in this mechanism was then studied by using the patch-clamp technique. First, addition of microfibril solvent did not lead to activation of membrane calcium channels showing that: *1*) the solvent is inactive on calcium channels, and *2*) HUVECs present a low basal activity of their membrane calcium channels, with no spontaneous activation over time (Fig. 1*K*). Conversely, addition of aortic microfibrils (0.15 μg/ml) produced a strong activation of calcium channels (Fig. 1*L*). Microfibril concentrations higher than 0.15 μg/ml were not used since preliminary experiments have shown that such concentrations induced too high activity of calcium channels, rapidly breaking the seal and ending the experiment. Intensity-voltage experiments were then performed, and unitary currents were measured at each imposed potential, resulting in a calculated conductance of the activated calcium channels in the range of 6 pS. Similar low conductance calcium channels (<16 pS) have previously been observed in endothelial cells and other cell types and involved in the response to elastin and growth factors (19, 20, 48, 66).

Action of Fibrillin-1 Fragments on $[Ca^{2+}]_i$

To verify whether the major component of microfibrils, i.e., fibrillin-1, was responsible for the effects triggered in HUVEC by aortic microfibrils, two overlapping fibrillin-1 RGD-containing fragments PF9 and PF14 were used. When compared with the control (Fig. 2*A*), PF9 did not modify HUVEC $[Ca^{2+}]_i$ at all the concentrations used (Fig. 2, *B–E*). On the contrary, PF14 application triggered a clear dose-dependent elevation of

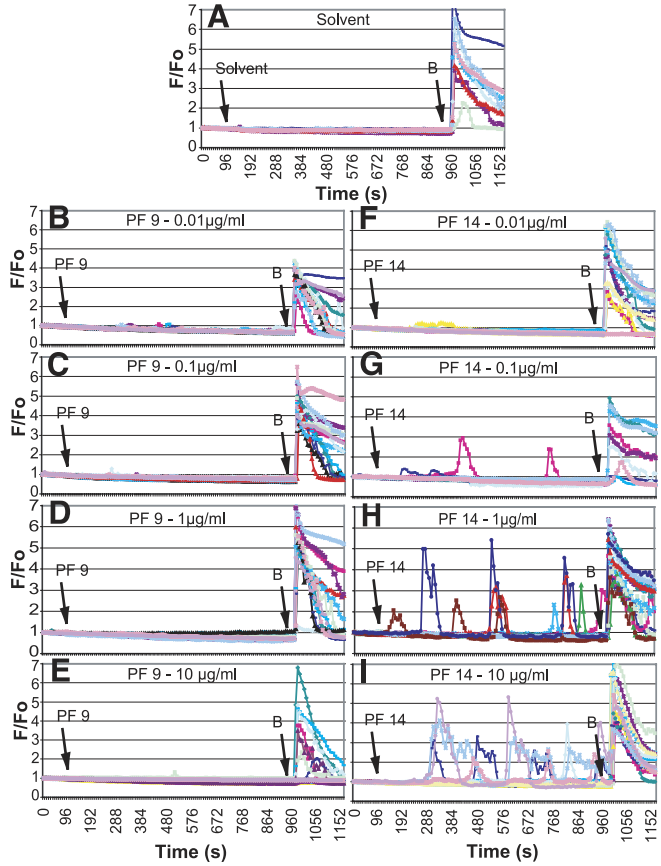

Fig. 2. Dose effect of fibrillin-1 fragments PF9 and PF14 on HUVEC intracellular free Ca^{2+} concentration ($[Ca^{2+}]_i$). Addition of solvent (*A*) or different concentrations of PF9 (*B–E*) or PF14 (*F–I*). B, bradykinin (1 μmol/l). Representative experiments are presented. In each case, n = 30–45 cells from at least 3 different cell cultures.

$[Ca^{2+}]_i$ in these cells. The fluorescence peaks appearing after addition of PF14 reached a value up to 2- to 5-fold the initial fluorescence level at the highest concentrations (Fig. 2, *F–I*). Also, some cells exhibited a unique fluorescence peak produced by PF14 (5–10% of the cells at 0.01–0.1 μg/ml PF14 ; ≈25% at 1 μg/ml PF14; ≈15% at 10 μg/ml PF14), while other cells responded several times by fluorescence peaks (≈0% at 0.01–0.1 μg/ml PF14; ≈15% at 1 μg/ml PF14; ≈30% at 10 μg/ml PF14). The average values of calcium peaks were in the ranges of 2.0 ± 0.4- to 2.6 ± 1.0-fold at 0.01–0.1 μg/ml PF14 and 4.2 ± 0.4- to 4.9 ± 0.2-fold at 1–10 μg/ml PF14. It was observed, however, that some cells did not respond to PF14 (≈90% at 0.01–0.1 μg/ml PF14; ≈55–60% at 1–10 μg/ml PF14) within the time window of the experiment, whereas 1 μmol/l bradykinin (a reference activator of endothelial $[Ca^{2+}]_i$) triggered a strong increase in $[Ca^{2+}]_i$ in most cells, confirming that HUVEC were functional even when nonresponding to PF14 (Fig. 2). Similar effect of PF9 and PF14 were also obtained in BAECs, which were responsive for ≈30% of them. However, the calcium peak amplitudes induced by 1 μg/ml PF14 (ranging from 1.2- to 3.4-fold, peak mean value: 2.4 ± 0.3-fold) were of lower amplitude in these cells than in HUVECs (online supplemental Fig. 1, *A–C*). Nevertheless, these results suggest that PF14-induced $[Ca^{2+}]_i$ signaling is a general mechanism in endothelial cells.

To verify whether PF14 acts on $[Ca^{2+}]_i$ in a longer term, HUVEC, free calcium concentrations measured by using the dye Fura-2 were compared before and 24 h after addition of 1 μg/ml PF14 to the cell culture medium. No calcium peak could be observed, and $[Ca^{2+}]_i$ values were not significantly changed by the treatment: 109 ± 21 nM at time 0 h and after 24 h, 143 ± 23 nM in the presence of solvent and 138 ± 19 nM in the presence of PF14 (n = 29–32 cells in each group, paired comparisons performed using one-way ANOVAs, $P > 0.25$ for the three comparisons). Our results suggest that PF14 does not durably modify endothelial free calcium concentration.

Similar to the effects previously observed in elastin-stimulated HUVECs (19), the calcium increases in response to microfibrils or PF14 were often asynchronous and of various amplitudes (no response to eightfold, single or multiple peaks) from cell to cell. This is possibly due the short time window of the experiment or, alternatively, to the presence of different endothelial cell subpopulations (our cultures being made of pooled cells from several individuals) differing from each other by the phase in the cell cycle or the receptor allele or expression level, as suggested by the existence of a genotype-dependent expression of endothelial NO synthase alleles (62). PF9 or PF14 (1 μg/ml;≈26 nM) were used in all further experiments.

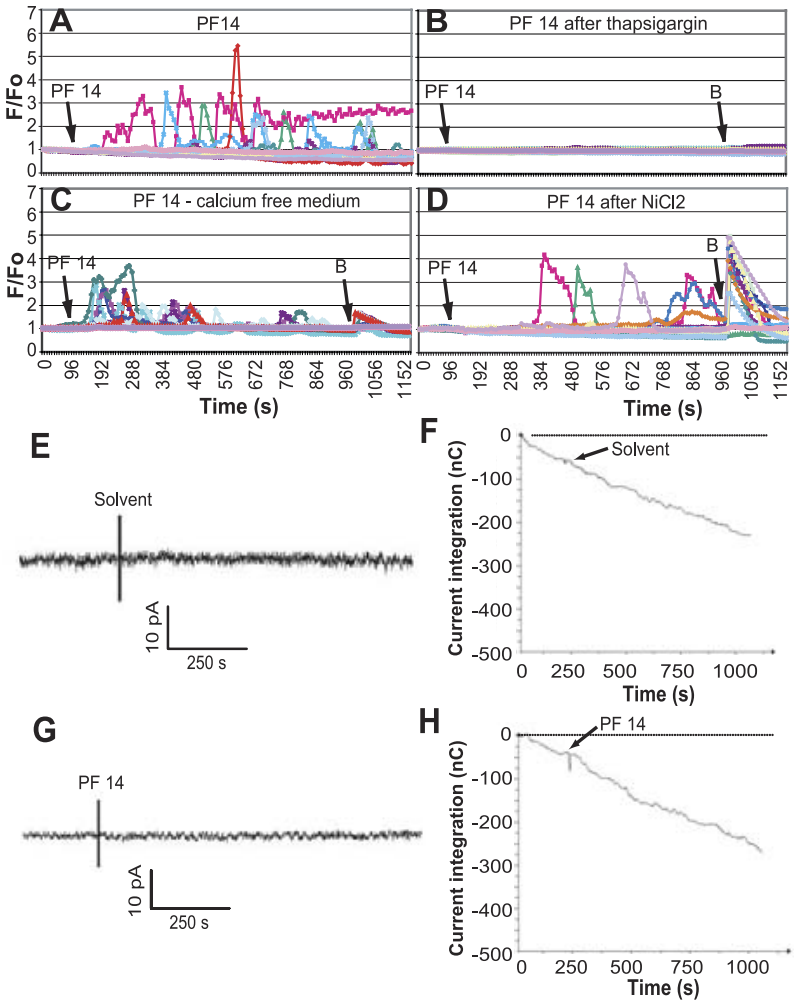

Fig. 3. Calcium origin in PF14-induced $[Ca^{2+}]_i$ elevations in HUVECs. Effect of PF14 (1 μg/ml) alone (*A*), after thapsigargin (1 μmol/l) (*B*), and bathing in calcium-free medium (C) or $NiCl_2$ (1 mmol/l) (*D*). B, bradykinin (1 μmol/l). n = 30–45 cells in each case. Effect of solvent (*E*, *F*; n = 5) or PF14 (1 μg/ml) (*G*, *H*; n = 10) on membrane calcium channels, recorded in patch-clamp experiments. Representative experiments are presented.

Origin of Calcium Leading to PF14-Triggered $[Ca^{2+}]_i$ Elevation in HUVECs

The question of the origin of the calcium mobilized by PF14 stimulation was then raised. When compared with control, emptying of the intracellular calcium stores by thapsigargin prevented PF14 to induce a $[Ca^{2+}]_i$ increase, suggesting a major role of the intracellular calcium stores in PF14 signaling (Fig. 3, *A* and *B*). This result was supported by another series of experiments aiming at the verification of the role of extracellular calcium influx in the PF14-induced $[Ca^{2+}]_i$ elevation. Placing the cells in a calcium-free medium; i.e., preventing calcium influx in the cells, had little effect on the general profile of $[Ca^{2+}]_i$ increases induced by PF14, except for a progressive decrease with time in the calcium peak sizes (Fig. 3*C*). This decrease is likely a side effect of bathing the cells in calcium-free medium, which induces a progressive emptying of the intracellular calcium stores (41) and therefore reduces the quantity of calcium that can be mobilized from the stores over time.

Also, blockade of HUVEC calcium channels by nickel chloride did not substantially inhibit PF14-induced elevation of $[Ca^{2+}]_i$ (Fig. 3*D*). This feature confirmed that the origin of the calcium mobilized by PF14 was mainly from the intracellular calcium stores, while extracellular calcium influx took a modest part, if any, in this mechanism. To further verify the minor involvement of extracellular calcium influx in the PF14-triggered elevation of $[Ca^{2+}]_i$, the effect of PF14 on the activity of membrane calcium channels was investigated using the patch-clamp technique in HUVECs. PF14 was not able to induce a calcium channel activity in 9 of 10 cells studied (Fig. 3, *E–H*), confirming the weak involvement of calcium influx.

Receptors and Signaling Pathways Activated by Fibrillin-1 Fragment PF14

To uncover the receptors involved in the PF14-induced calcium signaling pathway, a mutated form of PF14, PF14-RGA, in which the RGD sequence was replaced by RGA (which does not bind to integrins), was applied to the cells. As opposed to the clear response to PF14 (Fig. 4*A*), PF14-RGA did not trigger any response from HUVECs (Fig. 4*B*), suggesting an implication of integrins in the signal transduction. This was supported by the results from other experiments using

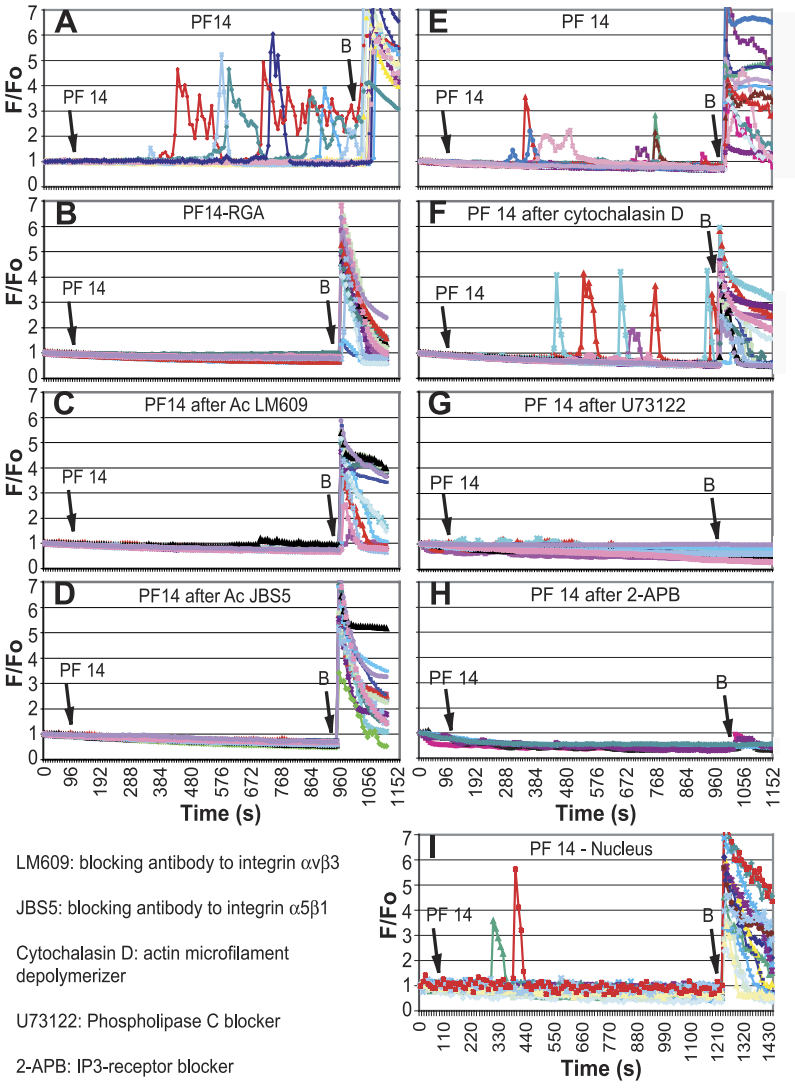

Fig. 4. PF14-activated receptors and signaling pathways mediating $[Ca^{2+}]_i$ elevations in HUVECs. PF14 (1 μg/ml) addition: alone (*A*, *E*), PF14-RGA (*B*), plus LM609 (1 μg/ml) (*C*), plus JBS5 (1 μg/ml) (*D*), or after cytochalasin-D (1 μmol/l) (*F*), U73122 (1 μmol/l) (*G*), or 2-APB (50 μmol/l) (*H*). *I*: effect on nuclear $[Ca^{2+}]$ (confocal microscopy). B, bradykinin (1 μmol/l). Representative experiments are presented. n = 30–45 cells in each case.

blocking antibodies to integrins αvβ3 and α5β1. Both antibodies abolished the response of HUVEC to PF14, suggesting the implication of the two above cited integrins in the transduction of the PF14 signal and suggesting that both integrins are needed for PF14 signaling (Fig. 4, *C* and *D*). The involvement of αvβ3 and α5β1 in PF14 signaling was further verified by using siRNA-mediated downregulation of these integrins. HUVEC transfection by siRNAs targeting either αv or α5 induced a substantial drop of the content of these integrin subunits in the cells (Fig. 5, *A*, *C*, and *D*) and strongly decreased, if not abolished, in both cases the cell response to PF14 (Fig. 5, *B* and *E*). This confirmed the implication of these two integrins in the transduction of the PF14 signal, which was also supported by the fact that classical ligands of αvβ3 (vitronectin) and α5β1 (fibronectin) produced the same type of calcium responses than those induced by PF14 in HUVECs (online supplemental Fig. 2).

The signaling pathway leading to PF14-induced elevation of $[Ca^{2+}]_i$ was then studied. When compared with control, depolymerization of actin microfilaments by cytochalasin D did not significantly modify HUVEC response to PF14 (Fig. 4, *E* and *F*), suggesting that PF14 signaling is not a mechanotransduction process mediated by integrin-connected actin microfilaments. However, since integrins are known to activate the Src

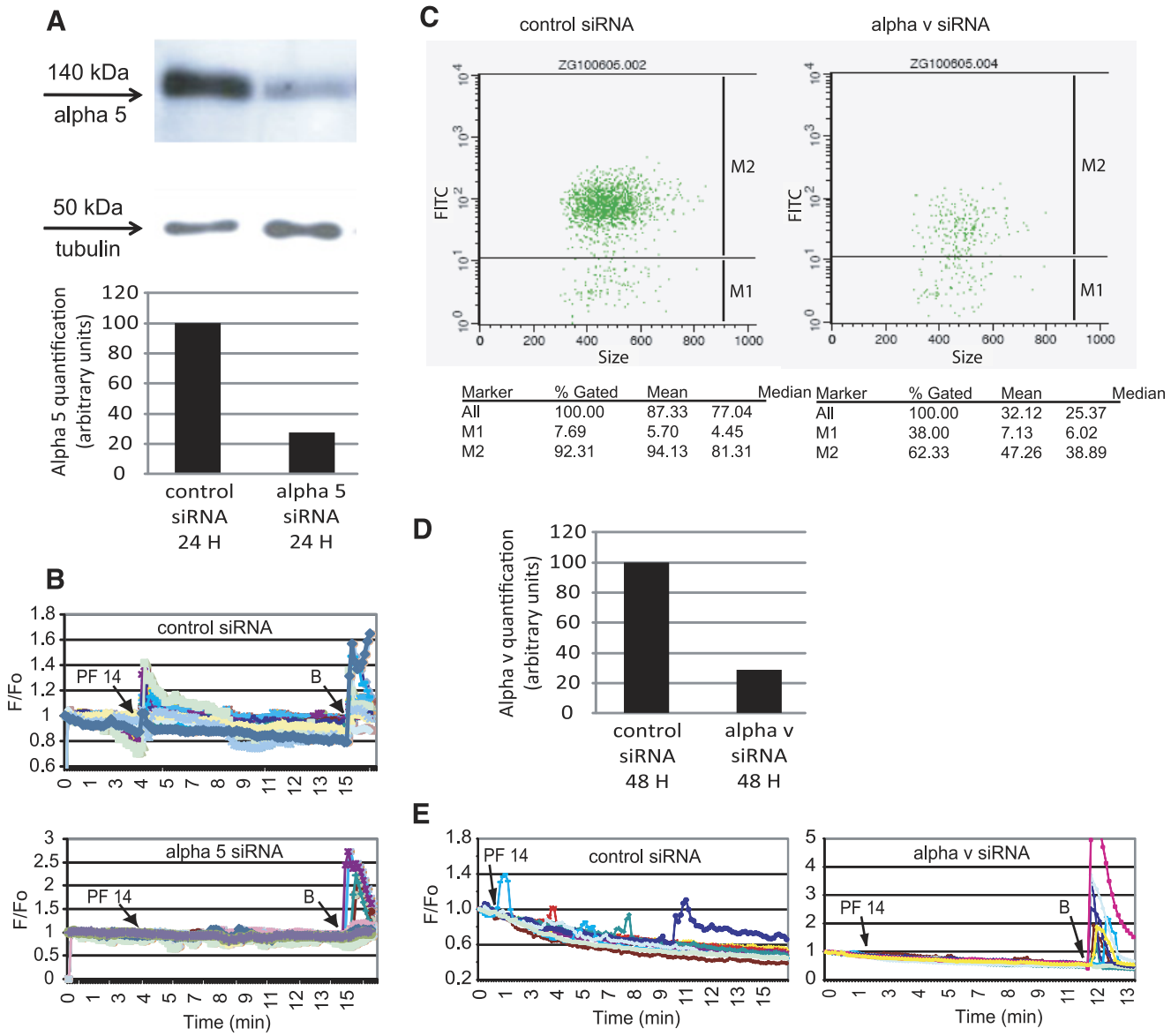

Fig. 5. Effects of small interfering RNA (siRNA) targeting of integrin subunits αv and α5 on $[Ca^{2+}]_i$ elevations induced by PF14 in HUVECs. Western blot and related quantification compared with tubulin of α5 (*A*) and effects of 1 μg/ml PF14 on $[Ca^{2+}]_i$ (*B*) in HUVECs transfected with control or α5 siRNAs. Flow cytometry analysis (*C*) and estimation of relative quantity (*D*) of αv, and effects of 1 μg/ml PF14 on $[Ca^{2+}]_i$ (*E*) in HUVECs transfected with control or αv siRNAs. In *C*, the graphs present the number of cells negative (M1) or positive (M2) for αv after transfection with control (*left*) or αv (*right*) siRNAs. Quantitative analyses are provided in the corresponding tables: Mean = mean fluorescence per cell ; % Gated = cell percentage in the group. When compared with the cells transfected with control siRNA, αv-positive cells were present in a lower percentage and expressed less αv after transfection with αv siRNA. PF14-induced $[Ca^{2+}]_i$ increases were of lower amplitudes in HUVECs transfected with control siRNA than in untransfected cells (Fig. 2), probably as a consequence of the cell transfection processes. B, bradykinin (1 μmol/l). The experiments were duplicated.

kinase, which subsequently activates phospholipase C (PLC) (31), we have also investigated this signaling pathway. When PLC was blocked by U73122, the PF14-induced $[Ca^{2+}]_i$ elevation was abolished, suggesting an involvement of at least one of the reaction products of PLC as a signaling molecule (Fig. 4*G*). Since inositol-1,4,5-trisphosphate (IP_3), a major reaction product of PLC, is classically known to trigger a release of calcium from the intracellular stores through binding to the IP_3 receptor present at the surface of the endoplasmic reticulum (8), the effects of IP_3-receptor blockade with 2-APB were evaluated. In this condition, PF14 was unable to trigger any increase in $[Ca^{2+}]_i$ in HUVEC, suggesting that IP_3 was the second messenger responsible for intracellular calcium store release (Fig. 4*H*). Finally, it has to be noted that, using confocal fluorescence microscopy, PF14 was also found to increase nuclear free calcium level in HUVECs (Fig. 4*I*).

Effect of PF14 on HUVEC Adhesion, Proliferation, and Migration

After it was demonstrated that PF14 was able to trigger calcium signaling in HUVECs, it was found necessary to investigate the effects of cell-fibrillin-1 fragment interaction on several cell functions; i.e., adhesion, migration, and proliferation.

A first set of experiments showed that fibronectin, PF9, and PF14 promoted a similar substantial dose-dependent adhesion of HUVECs, except for the highest dose used, for which fibronectin became slightly more effective than both PF9 and PF14 (Fig. 6*A*).

Since $[Ca^{2+}]_i$ is known to be involved in the regulation of cell proliferation and migration (8, 50), we have then verified whether the PF14-induced $[Ca^{2+}]_i$ increase impacts on these biological activities in HUVECs. The effects of BSA, PF9, and PF14 (10 μg/ml) on HUVEC transwell migration were assessed in Boyden chambers. These experiments showed that only PF14 was haptotactic and triggered a transmigration of HUVECs significantly different from the controls in the range of +65% (Fig. 6*B*). In addition, the effects of PF14 and PF9 on HUVEC proliferation was assessed by the trypsinization and direct cell counting method: only PF14 was found active, since the proliferation rate was +108% 48 h after addition of PF14 (1 μg/ml), while it was only +61% after addition of PF9 (1 μg/ml) and +66% in the presence of solvent alone (one-way ANOVA, $P \leq 0.05$) (Fig. 7*A*). The enhancement of cell proliferation by PF14 was then verified by using the WST-1 colorimetric method: HUVEC proliferation rate at 48 h was significantly higher after addition of PF14 (1 μg/ml) (+125% after 48 h) than after addition of solvent alone (+100%) (one-way ANOVA, $P \leq 0.05$) (online supplemental Fig. 1*D*). This is consistent with the significantly increased cell proliferation rate induced by aortic microfibrils (0.5 μg/ml) after 48 h, which reached +70% after addition of microfibrils and only +35% after addition of the solvent alone (one-way ANOVA, $P \leq 0.05$) (Fig. 7*A*). Finally, the effects of fibrillin-1 fragments on migration were further investigated in wound healing assays. After 8 h, only PF14 (1 μg/ml) induced a significantly higher wound closure (51%) than in control conditions with solvent alone (37%) (one-way ANOVA, $P < 0.05$) (Fig. 7, *B* and *C*).

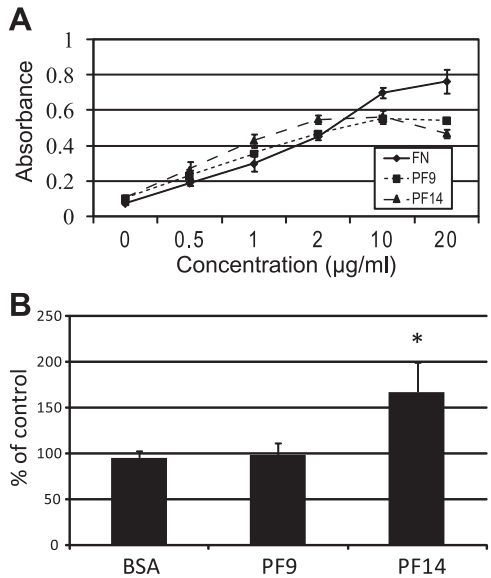

Fig. 6. Adhesion and transmigration of HUVEC in response to fibrillin-1 fragments PF9 and PF14. *A*: dose-dependent attachment of HUVECs to fibrillin-1 fragments PF9, PF14, and full-length human fibronectin ($n = 6$ in each case). *B*: transmigration of HUVEC when the underside of the Boyden chamber inserts was precoated with 10 μg/ml BSA, PF9, or PF14 ($n = 3$ in each case). *Significantly different from the control (uncoated underside of the Boyden chamber). Data are means ± SE.

DISCUSSION

MFS, caused by mutations in the fibrillin-1 gene, raises the question of knowing whether microfibrillar components are able to trigger intracellular signaling events that would be missing in case of genetic anomalies, potentially altering the developmental process. To support this idea, microfibrils and RGD-containing fibrillin-1 fragments are already known to enhance adhesion, spreading, and migration of several cell types (5, 6, 14, 47, 53, 54, 61, 70). Further support to this hypothesis was provided by *1*) evidence that mice mutated for other microfibrillar components, e.g., fibulin-5 or emilin-1, have severe anomalies of vascular development and structure (51, 73, 74), and *2*) the facts that mutations in the other main component of elastic fibers, elastin, cause Williams syndrome, and elastin fragments and tropoelastin have already been shown to influence Ca^{2+} signaling, proliferation, and other functions in vascular and other types of cells (17, 19, 27, 28, 33, 49, 68).

Here, we have shown that aortic microfibrils induced a substantial dose-dependent elevation of cytoplasmic and nuclear free calcium levels in endothelial cells. In particular, the rise in nuclear calcium level is known to modulate the activity of transcription factors and stimulate gene expression and cell proliferation (57) and may explain, at least in part, the increased cell proliferation triggered by microfibrils. To know which component of microfibrils was responsible for this effect, we studied the action of two RGD-containing overlapping fragments of their main component fibrillin-1, i.e., fragments PF9 and PF14. Although PF14 contains a wider sequence than PF9 on the NH_2-terminal side of the RGD, both fragments promote in vitro adhesion of fibroblasts (5, 6) and, according to the present experiments and previous results (70), endothelial cells. However, only PF14, not PF9, induced a substantial dose-dependent $[Ca^{2+}]_i$ increase in HUVECs, although

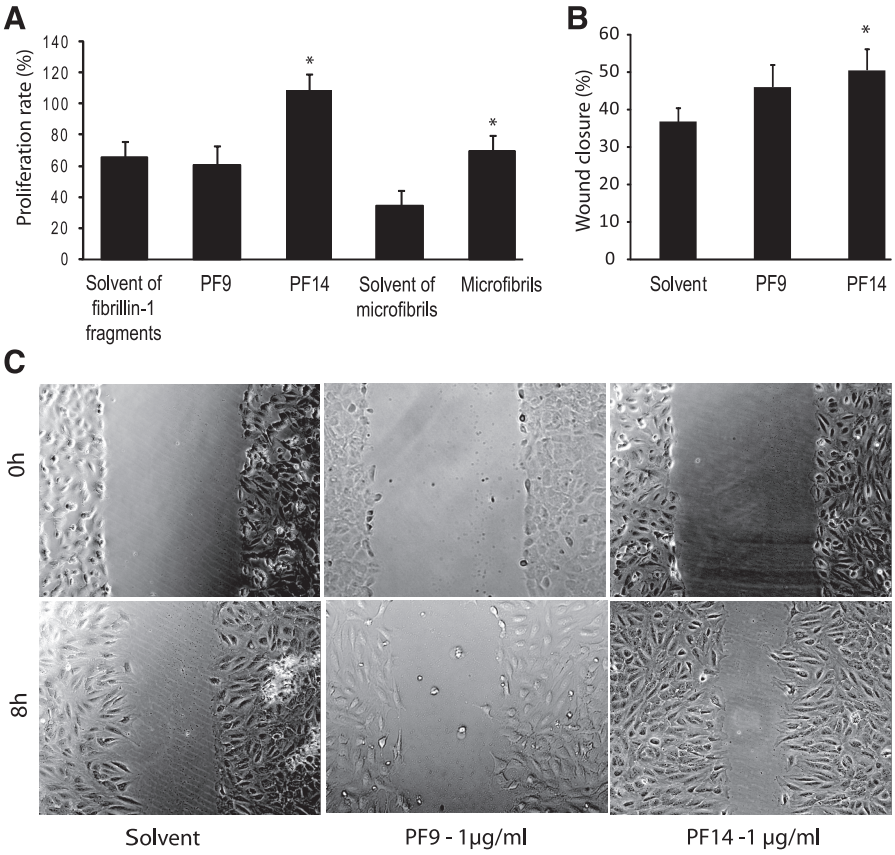

Fig. 7. Effect of PF9 and PF14 on HUVEC proliferation and wound healing. *A*: PF9 (1 μg/ml), PF14 (1 μg/ml), and aortic microfibrils (0.5 μg/ml) effects on HUVEC proliferation after 48 h, evaluated by cell counting ($n = 4–8$ dishes per group). *B*, *C*: effect of PF9 and PF14 (1 μg/ml) after 8 h on wound healing assays in HUVEC cultures ($n = 6$). In *A* and *B*, values are means ± SE. One representative experiment is shown in *C*. *Significantly different from corresponding solvent (one-way ANOVA, $P \leq 0.05$).

lower than the rise induced by aortic microfibrils. The different responses induced by PF9 and PF14 confirm the importance of the amino acids on the NH_2-terminal side of the RGD sequence of PF14 for cell recognition and/or function, as suggested previously (6, 40). At least, the PF14 domains upstream of RGD are needed to stabilize the binding to α5β1 and facilitate α5β1 activation. If they are absent, the RGD domain cannot activate α5β1 (6). Here, PF14 exerted a RGD-dependent action on calcium signaling through its binding to integrins substantially expressed in endothelial cells: α5β1 and αvβ3, the latter being known to also bind to tropoelastin (7, 56, 59). Curiously, in our experiments, the blockade of each of these integrins totally inhibited the effect of PF14. This could be explained by the previously demonstrated cross-talk between αvβ3 and α5β1 integrin signaling pathways (36) and subsequent inhibition of angiogenesis by blockade of either of these two integrins (37). Alternatively, the simultaneous activation of both integrins might be necessary for PF14 signal transduction in HUVECs, as shown for the action of several angiogenic factors in the induction of endothelial cells migration (25).

The transduction of extracellular matrix signals that activate integrins is often mediated by the actin-based cytoskeleton (69). Here, no involvement of actin microfilaments was observed in PF14-induced calcium signaling in HUVECs, similar to what was shown with aortic microfibrils. However, sequential mobilization of PLC, IP_3, and intracellular calcium stores were demonstrated to be a major pathway activated by PF14 binding to integrins and leading to $[Ca^{2+}]_i$ increase. In addition, as opposed to the effects of aortic microfibrils, no clear calcium channel activation could be observed following HUVEC stimulation by PF14. This, together with the higher HUVEC response to aortic microfibrils than to PF14, suggests that microfibril-induced calcium signaling in these cells also involves either microfibrilar components other than fibrillin-1 or fibrillin-1 sequences that are not present in PF14.

Integrin activation by extracellular matrix proteins often leads to $[Ca^{2+}]_i$ elevation, which regulates many cellular events, including adhesion, migration, proliferation, and angiogenesis (8, 50, 64). The present experiments suggested that PF14-induced increase in cytoplasmic and nuclear calcium level enhanced, at least, HUVEC proliferation and migration. Since microfibrils anchor the aortic endothelial cells to the subendothelial elastic lamina in the embryo (14), microfibrillar components, including fibrillin-1, could be responsible for physiological endothelial calcium signaling at the onset of vessel formation. Endothelial dysfunction is an important contributor to MFS (12, 71), acting in synergy with vascular smooth muscle cell (VSMC) dysfunction. Among several potential effects, the calcium signaling induced by fibrillin-1 fragments in endothelial cells likely activates the production of NO, which is known to regulate different functions of smooth muscle cells, such as apoptosis and synthesis of matrix metalloproteases involved in aortic dissection and aneurysmal progression (21, 24, 72). Dysregulation of calcium signaling, due to a decrease in the availability of fibrillin-1 in mutated animals or patients, may then alter NO production and its signaling effects, as suggested by the decreased activity of the calcium-dependent endothelial NO synthase (eNOS) in the aorta of a Marfan mouse model (12). In MFS, fibrillin-1 impairment may therefore alter physiological fibrillin-1 signaling in endothelial

cells, contribute to the endothelial dysfunction leading to the disease (71), and directly account for the arterial anomalies.

ACKNOWLEDGMENTS

We thank Dr. Daniel V. Bax (currently at University of Sydney, Australia) for contribution to providing the fibrillin-1 PF9 and PF14 fragments and Dr. Yves Vandenbrouck (CEA, Grenoble, France) for design of siRNAs.

GRANTS

The authors also acknowledge the European Commission (contracts TELASTAR, 5th PCRD, number QLK6-CT-2001-00332; and ELAST-AGE, 6th PCRD, number LSHM-CT-2005-018960) for funding.

DISCLOSURES

No conflicts of interest, financial or otherwise, are declared by the author(s).

REFERENCES

1. **Babbin BA, Parkos CA, Mandell KJ, Winfree LM, Laur O, Ivanov AI, Nusrat A.** Annexin 2 regulates intestinal epithelial cell spreading and wound closure through Rho-related signaling. *Am J Pathol* 170: 951–966, 2007.
2. **Bailey SR, Polan JL, Munoz OC, Agrawal MC, Goswami NJ.** Proliferation and beta-tubulin for human aortic endothelial cells within gas-plasma scaffolds. *Cardiovasc Radiat Med* 5: 119–124, 2004.
3. **Balconi G, Dejana E.** Cultivation of endothelial cells: limitations and perspectives. *Med Biol* 64: 231–245, 1986.
4. **Baldock C, Koster AJ, Ziese U, Rock MJ, Sherratt MJ, Kadler KE, Shuttleworth CA, Kielty CM.** The supramolecular organization of fibrillin-rich microfibrils. *J Cell Biol* 152: 1045–1056, 2001.
5. **Bax DV, Bernard SE, Lomas A, Morgan A, Humphries J, Shuttleworth CA, Humphries MJ, Kielty CM.** Cell adhesion to fibrillin-1 molecules and microfibrils is mediated by alpha 5 beta 1 and alpha v beta 3 integrins. *J Biol Chem* 278: 34605–34616, 2003.
6. **Bax DV, Mahalingam Y, Cain S, Mellody K, Freeman L, Younger K, Shuttleworth CA, Humphries MJ, Couchman JR, Kielty CM.** Cell adhesion to fibrillin-1: identification of an Arg-Gly-Asp-dependent synergy region and a heparin-binding site that regulates focal adhesion formation. *J Cell Sci* 120: 1383–1392, 2007.
7. **Bax DV, Rodgers UR, Bilek MM, Weiss AS.** Cell adhesion to tropoelastin is mediated via the C-terminal GRKRK motif and integrin alphaV-beta3. *J Biol Chem* 284: 28616–28623, 2009.
8. **Berridge MJ, Lipp P, Bootman MD.** The versatility and universality of calcium signaling. *Nat Rev Mol Cell Biol* 1: 11–21, 2000.
9. **Bussiere CT, Wright GM, DeMont ME.** The mechanical function and structure of aortic microfibrils in the lobster *Homarus americanus*. *Comp Biochem Physiol A Mol Integr Physiol* 143: 417–428, 2006.
10. **Cain SA, Morgan A, Sherratt MJ, Ball SG, Shuttleworth CA, Kielty CM.** Proteomic analysis of fibrillin-rich microfibrils. *Proteomics* 6: 111–122, 2006.
11. **Carta L, Pereira L, Arteaga-Solis E, Lee-Arteaga SY, Lenart B, Starcher B, Merkel CA, Sukoyan M, Kerkis A, Hazeki N, Keene DR, Sakai LY, Ramirez F.** Fibrillins 1 and 2 perform partially overlapping functions during aortic development. *J Biol Chem* 281: 8016–8023, 2006.
12. **Chung AW, Au Yeung K, Cortes SF, Sandor GG, Judge DP, Dietz HC, van Breemen C.** Endothelial dysfunction and compromised eNOS/Akt signaling in the thoracic aorta during the progression of Marfan syndrome. *Br J Pharmacol* 150: 1075–1083, 2007.
13. **Davis EC.** Smooth muscle cell to elastic lamina connections in developing mouse aorta. Role in aortic medial organization. *Lab Invest* 68: 89–99, 1993.
14. **Davis EC.** Immunolocalization of microfibril and microfibril-associated proteins in the subendothelial matrix of the developing mouse aorta. *J Cell Sci* 107: 727–736, 1994.
15. **El-Hallous E, Sasaki T, Hubmacher D, Getie M, Tiedemann K, Brinckmann J, Batge B, Davis EC, Reinhardt DP.** Fibrillin-1 interactions with fibulins depend on the first hybrid domain and provide an adaptor function to tropoelastin. *J Biol Chem* 282: 8935–8946, 2007.
16. **Faury G.** Function-structure relationship of elastic arteries in evolution: from microfibrils to elastin and elastic fibres. *Pathol Biol (Paris)* 49: 310–325, 2001.
17. **Faury G, Garnier S, Weiss AS, Wallach J, Fulop T Jr, Jacob MP, Mecham RP, Robert L, Verdetti J.** Action of tropoelastin and synthetic elastin sequences on vascular tone and on free Ca2+ level in human vascular endothelial cells. *Circ Res* 82: 328–336, 1998.
18. **Faury G, Pezet M, Knutsen RH, Boyle WA, Heximer SP, McLean SE, Minkes RK, Blumer KJ, Kovacs A, Kelly DP, Li DY, Starcher B, Mecham RP.** Developmental adaptation of the mouse cardiovascular system to elastin haploinsufficiency. *J Clin Invest* 112: 1419–1428, 2003.
19. **Faury G, Usson Y, Robert-Nicoud M, Robert L, Verdetti J.** Nuclear and cytoplasmic free calcium level changes induced by elastin peptides in human endothelial cells. *Proc Natl Acad Sci USA* 95: 2967–2972, 1998.
20. **Garnier-Raveaud S, Usson Y, Cand F, Robert-Nicoud M, Verdetti J, Faury G.** Identification of membrane calcium channels essential for cytoplasmic and nuclear calcium elevations induced by vascular endothelial growth factor in human endothelial cells. *Growth Factors* 19: 35–48, 2001.
21. **Geng YJ, Wu Q, Muszynski M, Hansson GK, Libby P.** Apoptosis of vascular smooth muscle cells induced by in vitro stimulation with interferon-gamma, tumor necrosis factor-alpha, and interleukin-1 beta. *Arterioscler Thromb Vasc Biol* 16: 19–27, 1996.
22. **Giusti B, Porciani MC, Brunelli T, Evangelisti L, Fedi S, Gensini GF, Abbate R, Sani G, Yacoub M, Pepe G.** Phenotypic variability of cardiovascular manifestations in Marfan Syndrome. Possible role of hyperhomocysteinemia and C677T MTHFR gene polymorphism. *Eur Heart J* 24: 2038–2045, 2003.
23. **Graef T, Steidl U, Nedbal W, Rohr U, Fenk R, Haas R, Kronenwett R.** Use of RNA interference to inhibit integrin subunit alphaV-mediated angiogenesis. *Angiogenesis* 8: 361–372, 2005.
24. **Gurjar MV, Sharma RV, Bhalla RC.** eNOS gene transfer inhibits smooth muscle cell migration and MMP-2 and MMP-9 activity. *Arterioscler Thromb Vasc Biol* 19: 2871–2877, 1999.
25. **Hotchkiss KA, Ashton AW, Schwartz EL.** Thymidine phosphorylase and 2-deoxyribose stimulate human endothelial cell migration by specific activation of the integrins alpha 5 beta 1 and alpha V beta 3. *J Biol Chem* 278: 19272–19279, 2003.
26. **Hubmacher D, Tiedemann K, Reinhardt DP.** Fibrillins: from biogenesis of microfibrils to signaling functions. *Curr Top Dev Biol* 75: 93–123, 2006.
27. **Ito S, Ishimaru S, Wilson SE.** Effect of coacervated alpha-elastin on proliferation of vascular smooth muscle and endothelial cells. *Angiology* 49: 289–297, 1998.
28. **Jacob MP, Fulop T Jr, Foris G, Robert L.** Effect of elastin peptides on ion fluxes in mononuclear cells, fibroblasts, and smooth muscle cells. *Proc Natl Acad Sci USA* 84: 995–999, 1987.
29. **Jaffe EA, Nachman RL, Becker CG, Minick CR.** Culture of human endothelial cells derived from umbilical veins. Identification by morphologic and immunologic criteria. *J Clin Invest* 52: 2745–2756, 1973.
30. **Jiang X, Yang F, Tan H, Liao D, Bryan RM Jr, Randhawa JK, Rumbaut RE, Durante W, Schafer AI, Yang X, Wang H.** Hyperhomocystinemia impairs endothelial function and eNOS activity via PKC activation. *Arterioscler Thromb Vasc Biol* 25: 2515–2521, 2005.
31. **Jones NP, Peak J, Brader S, Eccles SA, Katan M.** PLCgamma1 is essential for early events in integrin signalling required for cell motility. *J Cell Sci* 118: 2695–2706, 2005.
32. **Judge DP, Dietz HC.** Marfan's syndrome. *Lancet* 366: 1965–1976, 2005.
33. **Kamoun A, Landeau JM, Godeau G, Wallach J, Duchesnay A, Pellat B, Hornebeck W.** Growth stimulation of human skin fibroblasts by elastin-derived peptides. *Cell Adhes Commun* 3: 273–281, 1995.
34. **Kielty CM, Sherratt MJ, Shuttleworth CA.** Elastic fibres. *J Cell Sci* 115: 2817–2828, 2002.
35. **Kielty CM, Whittaker SP, Grant ME, Shuttleworth CA.** Attachment of human vascular smooth muscles cells to intact microfibrillar assemblies of collagen VI and fibrillin. *J Cell Sci* 103: 445–451, 1992.
36. **Kim S, Harris M, Varner JA.** Regulation of integrin alpha vbeta 3-mediated endothelial cell migration and angiogenesis by integrin alpha5beta1 and protein kinase A. *J Biol Chem* 275: 33920–33928, 2000.
37. **Kim S, Bell K, Mousa SA, Varner JA.** Regulation of angiogenesis in vivo by ligation of integrin alpha5beta1 with the central cell-binding domain of fibronectin. *Am J Pathol* 156: 1345–1362, 2000.
38. **Kuo CL, Isogai Z, Keene DR, Hazeki N, Ono RN, Sengle G, Peter Bachinger H, Sakai LY.** Effects of fibrillin-1 degradation on microfibril ultrastructure. *J Biol Chem* 282: 4007–4020, 2007.

39. **Lamouille S, Mallet C, Feige JJ, Bailly S.** Activin receptor-like kinase 1 is implicated in the maturation phase of angiogenesis. *Blood* 100: 4495–4501, 2002.
40. **Lee SS, Knott V, Jovanovic J, Harlos K, Grimes JM, Choulier L, Mardon HJ, Stuart DI, Handford PA.** Structure of the integrin binding fragment from fibrillin-1 gives new insights into microfibril organization. *Structure* 12: 717–729, 2004.
41. **Lew PD, Monod A, Krause KH, Waldvogel FA, Biden TJ, Schlegel W.** The role of cytosolic free calcium in the generation of inositol 1,4,5-trisphosphate and inositol 1,3,4-trisphosphate in HL-60 cells. Differential effects of chemotactic peptide receptor stimulation at distinct Ca^{2+} levels. *J Biol Chem* 261: 13121–13127, 1986.
42. **Li DY, Faury G, Taylor DG, Davis EC, Boyle WA, Mecham RP, Stenzel P, Boak B, Keating MT.** Novel arterial pathology in mice and humans hemizygous for elastin. *J Clin Invest* 102: 1783–1787, 1998.
43. **Lillie MA, David GJ, Gosline JM.** Mechanical role of elastin-associated microfibrils in pig aortic elastic tissue. *Connect Tissue Res* 37: 121–141, 1998.
44. **Lu Y, Sherratt MJ, Wang MC, Baldock C.** Tissue specific differences in fibrillin microfibrils analysed using single particle image analysis. *J Struct Biol* 155: 285–293, 2006.
45. **Marque V, Kieffer P, Gayraud B, Lartaud-Idjouadiene I, Ramirez F, Atkinson J.** Aortic wall mechanics and composition in a transgenic mouse model of Marfan syndrome. *Arterioscler Thromb Vasc Biol* 21: 1184–1189, 2001.
46. **Mátyás G, Alonso S, Patrignani A, Marti M, Arnold E, Magyar I, Henggeler C, Carrel T, Steinmann B, Berger W.** Large genomic fibrillin-1 (FBN1) gene deletions provide evidence for true haploinsufficiency in Marfan syndrome. *Hum Genet* 122: 23–32, 2007.
47. **McGowan SE, Holmes AJ, Mecham RP, Ritty TM.** Arg-Gly-Asp-containing domains of fibrillins-1 and -2 distinctly regulate lung fibroblast migration. *Am J Respir Cell Mol Biol* 38: 435–445, 2008.
48. **Merle PL, Feige JJ, Verdetti J.** Basic fibroblast growth factor activates calcium channels in neonatal rat cardiomyocytes. *J Biol Chem* 270: 17361–17367, 1995.
49. **Mochizuki S, Brassart B, Hinek A.** Signaling pathways transduced through the elastin receptor facilitate proliferation of arterial smooth muscle cells. *J Biol Chem* 277: 44854–44863, 2002.
50. **Munaron L.** Intracellular calcium, endothelial cells and angiogenesis. *Recent Patents Anticancer Drug Discov* 1: 105–119, 2006.
51. **Nakamura T, Lozano PR, Ikeda Y, Iwanaga Y, Hinek A, Minamisawa S, Cheng CF, Kobuke K, Dalton N, Takada Y, Tashiro K, Ross J Jr, Honjo T, Chien KR.** Fibulin-5/DANCE is essential for elastogenesis in vivo. *Nature* 415: 171–175, 2002.
52. **Pezet M, Jacob MP, Escoubet B, Gheduzzi D, Tillet E, Perret P, Huber P, Quaglino D, Vranckx R, Li DY, Starcher B, Boyle WA, Mecham RP, Faury G.** Elastin haploinsufficiency induces alternative aging processes in the aorta. *Rejuvenation Res* 11: 97–112, 2008.
53. **Pfaff M, Reinhardt DP, Sakai LY, Timpl R.** Cell adhesion and integrin binding to recombinant human fibrillin-1. *FEBS Lett* 384: 247–250, 1996.
54. **Porst M, Plank C, Bieritz B, Konik E, Fees H, Dotsch J, Hilgers KF, Reinhardt DP, Hartner A.** Fibrillin-1 regulates mesangial cell attachment, spreading, migration and proliferation. *Kidney Int* 69: 450–456, 2006.
55. **Reber-Müller S, Spissinger T, Schuchert P, Spring J, Schmid V.** An extracellular matrix protein of jellyfish homologous to mammalian fibrillins forms different fibrils depending on the life stage of the animal. *Dev Biol* 169: 662–672, 1995.
56. **Rodgers UR, Weiss AS.** Integrin alpha v beta 3 binds a unique non-RGD site near the C-terminus of human tropoelastin. *Biochimie* 86: 173–178, 2004.
57. **Rodrigues MA, Gomes DA, Nathanson MH, Leite MF.** Nuclear calcium signaling: a cell within a cell. *Braz J Med Biol Res* 42: 17–20, 2009.
58. **Rosenbloom J, Abrams WR, Mecham R.** Extracellular matrix 4: the elastic fiber. *FASEB J* 7: 1208–1218, 1993.
59. **Ruegg C, Mariotti A.** Vascular integrins: pleiotropic adhesion and signaling molecules in vascular homeostasis and angiogenesis. *Cell Mol Life Sci* 60: 1135–1157, 2003.
60. **Sakai LY, Keene DR, Glanville RW, Bachinger HP.** Purification and partial characterization of fibrillin, a cysteine-rich structural component of connective tissue microfibrils. *J Biol Chem* 266: 14763–14770, 1991.
61. **Sakamoto H, Broekelmann T, Cheresh DA, Ramirez F, Rosenbloom J, Mecham RP.** Cell-type specific recognition of RGD- and non-RGD-containing cell binding domains in fibrillin-1. *J Biol Chem* 271: 4916–4922, 1996.
62. **Senthil D, Raveendran M, Shen YH, Utama B, Dudley D, Wang J, Wang XL.** Genotype-dependent expression of endothelial nitric oxide synthase (eNOS) and its regulatory proteins in cultured endothelial cells. *DNA Cell Biol* 24: 218–224, 2005.
63. **Short SM, Derrien A, Narsimhan RP, Lawler J, Ingber DE, Zetter BR.** Inhibition of endothelial cell migration by thrombospondin-1 type-1 repeats is mediated by beta1 integrins. *J Cell Biol* 168: 643–653, 2005.
64. **Stupack DG, Cheresh DA.** Integrins and angiogenesis. *Curr Top Dev Biol* 64: 207–238, 2004.
65. **Thurmond FA, Koob TJ, Bowness JM, Trotter JA.** Partial biochemical and immunologic characterization of fibrillin microfibrils from sea cucumber dermis. *Connect Tissue Res* 36: 211–222, 1997.
66. **Vaca L, Kunze DL.** Depletion of intracellular Ca^{2+} stores activates a Ca^{2+}-selective channel in vascular endothelium. *Am J Physiol Cell Physiol* 267: C920–C925, 1994.
67. **Vert JP, Foveau N, Lajaunie C, Vandenbrouck Y.** An accurate and interpretable model for siRNA efficacy prediction. *BMC Bioinformatics* 7: 520, 2006.
68. **Wachi H, Sugitani H, Murata H, Nakazawa J, Mecham RP, Seyama Y.** Tropoelastin inhibits vascular calcification via 67-kDa elastin binding protein in cultured bovine aortic smooth muscle cells. *J Atheroscler Thromb* 11: 159–166, 2004.
69. **Wiesner S, Legate KR, Fassler R.** Integrin-actin interactions. *Cell Mol Life Sci* 62: 1081–1099, 2005.
70. **Williamson MR, Shuttleworth A, Canfield AE, Black RA, Kielty CM.** The role of endothelial cell attachment to elastic fibre molecules in the enhancement of monolayer formation and retention, and the inhibition of smooth muscle cell recruitment. *Biomaterials* 28: 5307–5318, 2007.
71. **Wilson DG, Bellamy MF, Ramsey MW, Goodfellow J, Brownlee M, Davies S, Wilson JF, Lewis MJ, Stuart AG.** Endothelial function in Marfan syndrome: selective impairment of flow-mediated vasodilation. *Circulation* 99: 909–915, 1999.
72. **Xiong W, Knispel RA, Dietz HC, Ramirez F, Baxter BT.** Doxycycline delays aneurysm rupture in a mouse model of Marfan syndrome. *J Vasc Surg* 47: 166–172, 2008.
73. **Yanagisawa H, Davis EC, Starcher BC, Ouchi T, Yanagisawa M, Richardson JA, Olson EN.** Fibulin-5 is an elastin-binding protein essential for elastic fibre development in vivo. *Nature* 415: 168–171, 2002.
74. **Zanetti M, Braghetta P, Sabatelli P, Mura I, Doliana R, Colombatti A, Volpin D, Bonaldo P, Bressan GM.** EMILIN-1 deficiency induces elastogenesis and vascular cell defects. *Mol Cell Biol* 24: 638–650, 2004.
75. **Zhang H, Hu W, Ramirez F.** Developmental expression of fibrillin genes suggests heterogeneity of extracellular microfibrils. *J Cell Biol* 129: 1165–1176, 1995.